An In Vitro Comparison of the Effects of the Iron Chelating Agents, CP94 and Dexrazoxane, on Protoporphyrin IX Accumulation for Photodynamic Therapy and/or Fluorescence Guided Resection

Emma Blake*, James Allen and Alison Curnow

Clinical Photobiology, Peninsula College of Medicine and Dentistry, University of Exeter, Knowledge Spa, Royal Cornwall Hospital, Truro, Cornwall, UK

*Corresponding author **e-mail**: emma.blake@pms.ac.uk (Emma Blake)

ABSTRACT

Photodynamic therapy (PDT) utilizes the combined interaction of a photosensitizer, light and molecular oxygen to ablate tumor tissue. Maximizing the accumulation of the photosensitizer protoporphyrin IX (PpIX) within different cell types would be clinically useful. Dermatological PpIX-induced PDT regimes produce good clinical outcomes but this currently only applies when the lesion remains superficial. Also, as an adjuvant therapy for the treatment of primary brain tumors, fluorescence guided resection (FGR) and PDT can be used to highlight and destroy tumor cells unreachable by surgical resection. By employing iron chelators PpIX accumulation can be enhanced. Two iron chelating agents, 1,2-diethyl-3-hydroxypyridin-4-one hydrochloride (CP94) and dexrazoxane, were individually combined with the porphyrin precursors aminolevulinic acid (ALA), methyl aminolevulinate (MAL) and hexyl aminolevulinate (HAL). Efficacies of the iron chelating agents were compared by recording the PpIX fluorescence in human squamous epithelial carcinoma cells (A431) and human glioma cells (U-87 MG) every hour for up to 6 hours. Coincubation of ALA/MAL/HAL with CP94 resulted in a greater accumulation of PpIX compared to that produced by coincubation of these congeners with dexrazoxane. Therefore the clinical employment of iron chelation, particularly with CP94 could potentially increase and/or accelerate the accumulation of ALA/MAL/HAL-induced PpIX for PDT or FGR.

INTRODUCTION

Photodynamic therapy (PDT) is a clinical treatment resulting from the interaction of a photosensitizer, molecular oxygen and light of a specific wavelength. When all three components are combined simultaneously in sufficient amounts they result in the production of singlet oxygen and other free radicals causing diseased cells to undergo cell death through necrosis or apoptosis (1). An increased or excessive amount of photosensitizer would be clinically useful and so research is taking place to try to increase photosensitizer accumulation during PDT with a view to ultimately enhancing clinical efficacy.

The prodrugs aminolevulinic acid (ALA), methyl aminolevulinate (MAL) and hexyl aminolevulinate (HAL) are porphyrin-inducing precursors of the endogenous photosensitizer protoporphyrin IX (PpIX) produced via the heme biosynthesis pathway in nucleated cells in humans. Usually in cells, following PpIX production the next stage in the pathway is the insertion of ferrous iron (Fe^{2+}) under the action of the ferrochelatase enzyme (2), to convert PpIX into heme, with the presence of free heme acting as a negative feedback mechanism limiting the production of any further ALA (3). However, the exogenous introduction of large amounts of ALA/MAL/HAL bypasses this negative feedback loop and there is a resultant accumulation of heme and heme precursors in the cell. Notably, the conversion of PpIX to heme by ferrochelatase is relatively slow which causes PpIX to temporarily accumulate within cells (4). In addition, in diseased cells some enzymes within the heme biosynthesis pathway are over or under expressed favoring the continual production of PpIX (5-7).

The first results from a clinical trial utilizing ALA-induced PpIX photodynamic therapy were reported just over 20 years ago (8) and since then PpIX-induced PDT for a variety of cancers has been investigated. Topically it can be used for the treatment of a number of

dermatological indications including the most common form of skin cancer, basal cell carcinoma (BCC). Although PpIX-induced PDT produces good clinical outcomes and excellent cosmesis for the thinner, superficial BCCs (sBCC), efficacy for the treatment of thicker nodular BCCs (nBCC) remains lower than conventional surgical excision (9). For patients presenting with nBCC lesions that are large, multiple and/or on cosmetically sensitive sites (10), surgical excision can be a disfiguring and distressing experience. Therefore, enhancement of PpIX-induced PDT for these thicker lesions would be beneficial.

Another promising application of PpIX accumulation within cancer cells is within human brain tumor cells. Human glioblastomas are aggressive primary brain tumors which remain the most common form of this malignancy (11) and problematic to treat given their infiltrative and mobile characteristics (12). Conventional treatments for brain tumors include surgery, radiotherapy and chemotherapy. Although these conventional therapies are potentially curative, the 5 year survival rates remain below 5%, with approximately 80% of reoccurrences occurring within 2 cm of the surgically resected margin (13). Activated PpIX, under light of a specific wavelength, has the ability to fluoresce and in 1998 Stummer *et al.* observed a fluorescence ratio of 5:1 between malignant and normal tissue *in vitro* (14). Utilizing a technique termed fluorescence guided resection (FGR) (15); surgeons can exploit PpIX's natural fluorescent properties enabling greater precision in the removal of brain tumors (16, 17). In addition to FGR, PpIX-induced PDT, as an adjuvant therapy, can be used to destroy residual tumor tissue unreachable by surgical resection. Improvement of PpIX accumulation within glioblastoma cells for the application of FGR and/or PDT could potentially improve prognosis, prolong time interval to tumor recurrence and vitally improve quality of life.

It has been shown that PpIX accumulation can be enhanced by employing iron chelation (18). An iron chelating agent can temporarily remove free Fe^{2+} from the system, inhibiting its insertion into PpIX, thus preventing the formation of heme and as a result PpIX accumulates in the cell (19). Iron chelating agents which have been investigated in the past include ethylenediamine tetra acetic acid (EDTA) (20) and desferrioxamine (DFO) (21) Liu *et al.* (2004) (2) concluded that a non-specific metal chelator (with the potential to inhibit ferrochelatase activity), calcium-disodium edentate ($CaNa_2$ EDTA) combined with ALA increased PpIX accumulation and photosensitization in Hep-2 cells. In addition to cell culture tests they treated 12 non-melanoma skin cancer patients with ALA combined with $CaNa_2$ EDTA-PDT and found greater depth of penetration than compared to ALA-PDT alone. From these experiments they postulated that if $CaNa_2$ EDTA combined with ALA was used clinically for the treatment of cutaneous cancers the depth of PpIX penetration and therefore clinical outcome could be improved (2). DFO has greater specificity for iron than EDTA and research by our group has shown 1,2-diethyl-3-hydroxypyridin-4-one hydrochloride (CP94) to be significantly superior to DFO in the enhancement of PpIX accumulation using ALA and MAL in fetal lung fibroblasts and squamous carcinoma cells (19).

Dexrazoxane (ICRF-187) is a clinically approved anthracycline-induced cardioprotective agent which has been used for more than 20 years (22). Dexrazoxane's proposed mechanism of action is that it readily penetrates cell membranes, is intracellularly converted into two one-ring open intermediates followed by the production of ADR-925, which can either remove iron from the iron-anthracycline complex or bind to free iron (22). It has been reported that all three hydrolysis products are good iron-chelating agents (23) and dexrazoxane itself is therefore known as an iron chelating prodrug.

These findings suggest that dexrazoxane may be used clinically as a successful iron chelating prodrug to enhance PpIX accumulation and to our knowledge has not previously been investigated for this purpose. This study therefore compares the effects of the iron chelating agents CP94 and dexrazoxane, on the accumulation of PpIX within human squamous epithelial cells and human glioma cells *in vitro* with ALA, MAL and HAL as the porphyrin precursors.

MATERIALS AND METHODS

Chemicals and cells

All reagents and chemicals were purchased from Sigma-Aldrich Chemical Company (Poole, UK) unless otherwise stated. U-87 MG (human glioblastoma-astrocytoma, epithelial-like) and A431 (human epithelial squamous carcinoma) cells were purchased from the European Collection of Cell Cultures (ECACC, Wiltsure, UK). Under aseptic conditions in a class II laminar flow cabinet, cells were cultured in Eagle's minimum essential medium (EMEM) with 10% fetal calf serum (FCS, standardized to give an iron concentration between 450 and 600 µg/100 g), 2% (200 mM) L-glutamine and 2% (200 U mL^{-1}) penicillin and (200 µg mL^{-1}) streptomycin solution. Stock solutions of ALA/MAL/HAL were prepared in phosphate buffered saline (PBS), adjusted to physiological pH (pH 7.4) using NaOH (0.5 mM), filter sterilized (0.22 µm Millipore) and stored at -20ºC for up to one month. Cells were grown in 5% CO_2 at 37ºC and left to grow until 70% confluent at which time cells were routinely passaged (every 3-5 days).

Iron chelator cytotoxicity

Before investigating PpIX accumulation the dark toxicity of each iron chelating agent was determined using the XTT (2,3-bis[2-Methoxy-4-nitro-5-sulfophenyl]-2H-tetrazololium-5-carboxyanilide inner salt) cell viability assay. This is a colorimetric assay based on the reduction of the XTT tetrazolium salt by mitochondrial dehydrogenase enzymes.

A431 and U-87 MG cells were seeded into multiwell plates at a density of 1 x 10^5 cells per mL (1 x 10^4 cells per well) and left to adhere overnight at 5% CO_2 and 37ºC. Under low light conditions the medium was aspirated from the wells and the cells washed with PBS in preparation for the addition of freshly prepared test solutions. Final concentrations of dexrazoxane and CP94 were prepared with modified EMEM (minus phenol red): dexrazoxane (50 and 150 µm) and CP94 (150 µm). A 100 µl volume of each test solution was added to the cells in triplicate wells. Control wells were also included which contained cells only incubated with modified EMEM. Once the test solutions had been added, cells were incubated for 3 hours in 5% CO_2 at 37ºC.

Following this incubation period, the medium containing the test solutions was removed from the wells and cells were washed three times with PBS. A volume of 120 µl serum free medium per well containing XTT was then added. The plate was returned to the incubator for a further 2 hours and following this, absorbance of the resulting color change was measured with a Synergy HT plate reader (BIO-TEK, Germany). Absorbance was read at 450 nm and 690 nm, with the 690 nm wavelength being used as a reference range and subtracted from the 450 nm reading. Measurements were represented as a percentage of the control cells, incubated with modified EMEM only.

PpIX fluorescence quantification

Cells were seeded into multiwell plates at a density of 1 x 10^5 cells per mL (1 x 10^4 cells per well) and left to adhere overnight at 5% CO_2 and 37ºC. Under low light conditions the medium was aspirated from the wells and the cells washed with PBS in preparation for the addition of freshly prepared test solutions. Final concentrations of ALA/MAL/HAL were prepared with modified EMEM (minus phenol red): ALA (250 µm) / MAL (1000 µm) / HAL (10 µm). To produce solutions of equal iron binding equivalence dexrazoxane was used at 50 µM and CP94 at a concentration of 150 µM. To compare equal molar concentrations dexrazoxane was also used at 150 µM. All concentration combinations were tested in quintuplicate on each plate in a minimum of three separate experiments conducted on separate days.

Under dark room conditions PpIX fluorescence quantification was conducted using a multi-well plate reader (Synergy HT, Bio-Tek, UK). Measurements were taken from the bottom of the wells with a 400 ± 30 nm excitation filter and a 645 ± 40 nm emission filter in place. Readings were taken every hour for a total of 6 hours and under dark room conditions to reduce photobleaching of PpIX. After/between each reading, plates were kept in the dark at 5% CO_2 and 37ºC.

Data analysis and statistics

The PpIX fluorescence measurements from the control cells not incubated with any test compound were used to remove natural cellular PpIX autofluorescence from all the other measurements made from the same plate. Following the determination of the presence of parametric data sets statistical significance between individual groups was determined using the Student's *t*-test and ANOVA was employed when considering differences between data sets.

RESULTS

Dark toxicity of CP94 and dexrazoxane

The dark toxicity of the two iron chelating agents, CP94 and dexrazoxane, incubated alone with squamous carcinoma (A431) and glioma (U-87 MG) cells was investigated (Fig 1). It was observed that both iron chelating agents produced similar results in each cell type with the Student's *t*-test revealing that at the concentrations tested no statistically significant toxicity was observed with either iron chelating agent, when compared to the same cell type incubated with modified EMEM alone (control group) (Fig 1).

The effect of CP94 and dexrazoxane on PpIX accumulation in squamous carcinoma (A431) cells

In the human epithelial carcinoma cells (A431) incubated with the prodrugs ALA/MAL/HAL with and without the iron chelators CP94 and dexrazoxane, PpIX fluorescence levels increased hourly and using an ANOVA with a post-test a significant linear trend was found ($p<0.01$, Figs 2a–2b). Comparison of ALA/MAL/HAL + CP94 with ALA/MAL/HAL alone (Figs 2a–2c) indicated that greater levels of PpIX fluorescence were detected in cells in the CP94 group and this difference was found to be statistically significant (ANOVA, $p<0.05$) with all three prodrugs. When cells incubated with ALA/MAL/HAL + dexrazoxane, at either concentration (50 µM or 150 µM), were compared to those incubated with ALA/MAL/HAL alone (Figs 2a–2c) using ANOVA to detect any significant difference ($p<0.05$) none was found. However, when using a Student's *t*-test between the prodrugs alone and the prodrugs + 150 µM dexrazoxane data sets, statistical significance was observed for the ALA/MAL/HAL + 150 µM dexrazoxane

treated cells at 2 hr (Fig 2a) / 1 hr (Fig 2b) / 3 hr (Fig 2c) respectively, and at all time points thereafter ($p<0.05$).

Comparison of ALA/MAL/HAL + CP94 with ALA/MAL/HAL + dexrazoxane (Figs 2a–2c) indicated that greater levels of PpIX fluorescence were detected in cells in the CP94 group and this difference was found to be statistically significant (ANOVA; with 50 μM dexrazoxane $p<0.001$, with 150 μM dexrazoxane $p<0.01$). Further analysis found significant enhancement in the ALA/MAL + CP94 treated cells compared to ALA/MAL + 50 μM dexrazoxane treated cells at every time point (Student's *t*-test, $p<0.05$; Figs 2a and 2b) and at a significance of $p<0.05$ after the first hour between HAL + CP94 and HAL + 50 μM dexrazoxane (Fig 2c). In addition, significant enhancement was observed between ALA/MAL/HAL + CP94 treated cells with ALA/MAL/HAL + 150 μM dexrazoxane for; ALA ($p<0.05$ at $\geq$ 1 hr), MAL ($p<0.05$ at $\geq$ 2 hr), HAL ($p<0.05$ at $\geq$ 0 hr).

In the cells incubated with ALA/MAL +/- CP94 or dexrazoxane (Figs 2a and 2b) the natural levels of PpIX detected, although similar, were greater when incubated with MAL +/- CP94 or dexrazoxane, at every time point. In the cells incubated with HAL alone and with HAL + 50 μM dexrazoxane, the levels of PpIX fluorescence were observed to decrease following 5 hours, whereas following 5 hours coincubation with HAL + CP94 or HAL + 150 μM dexrazoxane PpIX levels continued to increase (Fig 2c). Furthermore, the PpIX levels observed with 10 μM HAL were not as great as those produced by 250 μM ALA or 1000 μM MAL. Although the control results and ALA/MAL/HAL + CP94 results were comparable with our previous findings (24).

The enhanced levels of PpIX fluorescence detected could be represented as reduced incubation times (Fig 2d). Comparable levels of fluorescence to the cells incubated with ALA

alone at 6 hours could be achieved in ~ 4 hr 40 min with ALA + 50 μM dexrazoxane, in just over 3 hr with ALA + 150 μM dexrazoxane and in just over 2 hr with ALA + CP94 (approximately a third of the time required by ALA alone). Similar reductions in incubation times were observed with the MAL treated cells. Comparable levels of fluorescence to the cells incubated with MAL alone at 6 hours could be achieved in 5 hr with MAL + 50 μM dexrazoxane, in ~ 4 hr with MAL + 150 μM dexrazoxane and in just over 2 hr with MAL + CP94. Even greater reductions in incubation times were observed for the HAL treated cells. Comparable levels of fluorescence to the cells incubated with HAL alone at 6 hours could be achieved in ~ 3 hr with HAL + 50 μM dexrazoxane, in ~ 2 hr 20 min with HAL + 150 μM dexrazoxane and in just over 1 hr with HAL + CP94. Although, notably less PpIX fluorescence was observed when A431 cells were incubated with 10 μM HAL alone compared to incubation with either 250 μM ALA or 1000 μM MAL alone.

The effect of CP94 and dexrazoxane on PpIX accumulation in glioma (U-87 MG) cells

In human glioma cells (U-87 MG) incubated with the prodrugs ALA/MAL/HAL with and without the iron chelating agents CP94 and dexrazoxane, PpIX fluorescence levels increased hourly (Figs 3a–3c) and produced greater levels of PpIX fluorescence than the A431 cells with or without the iron chelating agents (Figs 2a–2c). For the U-87 MG cells, comparison of the prodrugs alone and the prodrugs with either iron chelating agent, using an ANOVA, revealed no statistically significant enhancement in PpIX fluorescence ($p<0.05$) trends (Figs 3a–3c).

However, using a Student's *t*-test to compare PpIX fluorescence levels in individual groups, when cells were treated with the prodrugs alone or the prodrugs with either iron chelator,

significant PpIX enhancements were found at specific time points. In Fig 3a, cells treated with ALA + CP94 at every time point produced statistically greater PpIX fluorescence than the ALA only treated cells ($p<0.05$). In addition, compared to treatment with ALA alone, cells treated with ALA + 50 μM dexrazoxane had statistically greater PpIX fluorescence between 5 and 6 hr and cells treated with ALA + 150 μM dexrazoxane had statistically greater PpIX fluorescence between 1–6 hr ($p<0.05$). Compared to treatment with ALA + 50 μM dexrazoxane, cells incubated with ALA + CP94 produced higher levels of PpIX fluorescence at the majority of time points investigated, with the exception of 2 hr. However, no statistically significant differences were observed between individual ALA + 150 μM CP94 or ALA + 150 μM dexrazoxane groups.

In the cells incubated with MAL +/- CP94 or dexrazoxane (Fig 3b), the levels of PpIX, although visually consistently greater when combined with CP94 were only significantly different to the MAL only controls and those treated with 50 μM or 150 μM dexrazoxane at 0 and 1 hr. In the cells incubated with HAL alone and with HAL + 50 μM dexrazoxane levels of PpIX fluorescence were observed to decrease following 5 hours, whereas following 5 hours incubation with HAL + CP94 or HAL + 150 μM dexrazoxane PpIX levels continue to increase (Fig 3c). In addition, following 4 hours plus incubation, levels of PpIX fluorescence were significantly greater when cells were incubated with HAL + 150 μM dexrazoxane compared to incubation with HAL + CP94 ($p<0.05$).

The enhanced levels of PpIX fluorescence detected could again be represented as reduced incubation times (Fig 3d). Comparable levels of fluorescence to the cells incubated with ALA alone at 6 hours could be achieved in ~ 4 hr 50 min with ALA + 50 μM dexrazoxane and in ~ 3 hr 30 min with either ALA + 150 μM CP94 or dexrazoxane. Following 6 hours incubation with MAL alone comparable levels of fluorescence were achieved at ~ 6 hr with MAL + 50 μM

dexrazoxane and in 5 hr 12 minutes with MAL + CP94. However, comparable levels of fluorescence to the cells incubated with MAL alone at 6 hours were not reached with MAL + 150 µM dexrazoxane. Greater reductions in incubation times were once again observed for the HAL treated cells. Comparable levels of fluorescence to the cells incubated with HAL alone at 6 hours could be achieved in ~ 3 hr 20 min with HAL + 50 µM dexrazoxane and in ~ 2 hr 40 min with either MAL + 150 µM CP94 or dexrazoxane. These findings in human glioma cells (Fig 3d) were therefore similar as those produced in human squamous epithelial carcinoma cells (Fig 2d) when employing ALA or HAL as the prodrug but not as marked when using MAL.

DISCUSSION

One of the major limitations of PpIX-induced FGR and PDT is the accumulation and localization of PpIX within tumor cells. Although it has been increasingly reported that PpIX accumulation can be enhanced with iron chelation (25), the use of which PpIX precursor and which iron chelating agent to administer for different cell types and which to take forward into clinical experimentation remains inconclusive.

This *in vitro* study was carried out to compare the increase in PpIX fluorescence, over a 6 hour time period, in human squamous epithelial carcinoma cells (A431) and human glioma cells (U-87 MG) after exogenous administration of ALA/MAL/HAL with and without the two iron chelating agents CP94 and dexrazoxane. CP94 was used because previous *in vitro* studies have shown CP94 to be significantly superior to the well-known iron chelator DFO (21) at increasing levels of PpIX (19). In addition, CP94 combined with ALA has been tested *in vivo*, with the PpIX fluorescence produced in rat colonic mucosa double that of ALA alone (25). An ongoing

clinical investigation using increasing concentrations of CP94 combined with ALA or MAL to carry out PDT on nBCCs which after 6 weeks are surgically excised, is currently being undertaken. Clinical assessment prior to excisions has so far demonstrated that using ALA + 40% CP94 produced a significantly greater clearance rate in nBCCs than with ALA-PDT alone (26). The clinical use of CP94 however remains experimental and non-licensed at the current time. However, dexrazoxane is already approved and used clinically, exerting its iron chelating properties successfully as a protective agent for anthracycline-induced cardiotoxicity. Therefore, comparing the iron chelating efficacies of CP94 and dexrazoxane with their ability to increase PpIX accumulation is useful, and to our knowledge this is the first study to investigate the combined interaction of any PpIX precursor with dexrazoxane.

In the human squamous epithelial carcinoma cells (A431) both CP94 and dexrazoxane treatment groups increased PpIX fluorescence when combined with the three prodrugs ALA/MAL/HAL, compared to each prodrug alone and markedly, CP94 produced significantly greater levels of PpIX accumulation when compared to dexrazoxane for each of the prodrugs tested. In addition, in A431 cells treated with CP94 and dexrazoxane, at both concentrations tested, the same amount of PpIX fluorescence normally produced during 6 hour incubation with ALA/MAL/HAL was produced within shorter time periods. Notably, this level of fluorescence was reached 3 times quicker when ALA and MAL were combined with CP94 and 6 times quicker when HAL was combined with CP94. Currently, dermatology PDT clinic drug-light-interval times are 4-6 hours for ALA and 3 hours for MAL (27). This time is important to allow for optimum levels of PpIX to accumulate and to produce an optimum ratio of photosensitizer accumulation between tumor and non tumor tissues (19). The results from this study suggest dermatology PDT clinics may benefit most from inclusion of CP94 in their treatment regimes to

firstly reduce incubation times resulting in a greater number of treatments being feasible in a day and thus reduced waiting times for patients and secondly to increase efficacy in applications requiring enhancement. However, use of the more clinically acceptable dexrazoxane may also produce some clinical benefits, and warrants further investigation.

In A431 cells it has been demonstrated here that CP94 is a greater enhancer of PpIX accumulation than both concentrations of dexrazoxane investigated, for each of the PpIX precursors tested. Notably, dexrazoxane was employed at two concentrations; 50 μM and 150 μM, whereas CP94 was only employed at 150 μM. This was done to take into account the different iron binding equivalences of the two iron chelating agents. Dexrazoxane is hexadentate meaning a single Fe molecule is coordinated by one chelator molecule in a 1:1 ratio. CP94 is bidentate meaning it binds iron in the ratio of 3:1. As a result the concentrations employed were chosen to produce solutions of equal iron binding equivalence (150 μM CP94 vs 50 μM dexrazoxane) and fairly compared equimolar concentrations of each iron chelating agent (150 μM) but in each case CP94 out performed dexrazoxane.

The end hydrolysis product of dexrazoxane, ADR-925 is a cyclic derivative of EDTA which has been investigated previously as an enhancer of PpIX-induced PDT (20). The polar nature of ADR-925, like that of EDTA prevents it from being able to cross cell membranes but this obstacle is overcome when dexrazoxane is employed instead of EDTA as its likely mode of transport is passive diffusion across cell membranes, similar to that shown for ICRF-159 (razoxane) (28). As CP94 and dexrazoxane can both readily enter cells one could postulate the decreased efficacy of dexrazoxane to increase PpIX accumulation compared to CP94, might be explained by dexrazoxane's conversion to its hydrolysis products. Physiological conditions studies (29, 30) have demonstrated that dexrazoxane is hydrolyzed to its one-ring open

intermediates with a $T_{1/2}$ of 9.3 hr at 37ºC and pH 7.4, whereas the final hydrolysis product ADR-925 was produced with a $T_{1/2}$ of 23 hr. In the present study incubation times of up to 6 hours only were employed but PpIX accumulation was still observed to occur at a greater level when each PpIX precursor was combined with dexrazoxane than incubation with each PpIX precursor alone. This could be explained by the observation that dexrazoxane can be enzymatically hydrolyzed, more rapidly, by dihydropyrimidine amidohydrolase (DHPase) to its one-ring open intermediates (31, 32), which like ADR-925 are also able to chelate iron. In addition, nonenzymatic metal-ion-promoted hydrolysis of dexrazoxane has also been reported (23, 33) in which it was suggested that both ferrous and ferric forms of iron are able to promote the hydrolysis of dexrazoxane or its open ring intermediates enhancing their iron-chelating potential.

In the human glioma cells (U-87 MG) it was again demonstrated that iron chelation with either agent significantly increased PpIX fluorescence when combined with the three prodrugs ALA/MAL/HAL, compared to each prodrug alone. These results are complementary to previous work conducted by ourselves (24) and also by others (34) who have considered the use of PpIX-induced FGR. Valdes *et al.* (2010) (34) suggested that although the use of ALA for FGR has shown promising results in previous clinical trials, due to heterogeneous staining and variation in PpIX production some tumor margins go undetected, proposing this may be remedied by combining FGR with iron chelation. In a recent study by Valdes *et al.* mice were implanted with xenograft U251-GFP Glioma tumor cells and administered with DFO once a day for 3 days prior to ALA administration producing a 50% increase in PpIX fluorescence relative to the control group (34).

Notably, in our study, at concentrations of equal binding equivalence (50 μM dexrazoxane vs 150 μM CP94) CP94 was a statistically greater enhancer of PpIX accumulation than dexrazoxane, when ALA or HAL were used as the PpIX precursor. With the prodrug MAL however these differences were less marked. However, at equimolar concentrations (150 μM) PpIX accumulation between the two iron chelating agents was similar, with the exception of coincubation with HAL where coincubation with dexrazoxane at 150 μM resulted in greater PpIX accumulation compared to coincubation of HAL with CP94. Nevertheless, the same amount of PpIX fluorescence normally produced during 6 hour incubation with HAL alone was produced in less than 3 hours when HAL was combined with either CP94 or 150 μM dexrazoxane. The *in vitro* results suggest that HAL coincubated with either iron chelator (CP94 or dexrazoxane) would most likely be the most favorable PpIX-induced therapy for the treatment of primary gliomas through FGR and/or PDT. However, unlike dermatology clinics where a reduced prodrug incubation period is highly favorable, in the surgical resection of brain tumors a reduced incubation period would take second place to producing the maximal amount of PpIX possible, given that successful tumor clearance is directly linked to the level of PpIX accumulated within malignant cells and is of major importance.

In mice implanted with glioma tumour cells with subsequent administration of DFO and ALA, 50% more PpIX fluorescence was recently demonstrated, relative to the control group (34). As previously mentioned CP94 has been shown to be significantly superior to DFO in enhancing PpIX accumulation (19) and CP94 has the ability to cross the blood-brain barrier (BBB) (35). *In vivo* animal studies should therefore investigate the hypothesis that exogenous systemic administration of ALA/MAL/HAL with CP94 in malignant glioma tumours could significantly increase PpIX fluorescence. In addition, tumour-to-normal tissue selectivity should

also be investigated *in vivo*. In the surgical resection of brain tumours sparing normal tissue to maximize post-operational quality of life is an important consideration therefore achieving maximal tumour-to-normal PpIX selectivity is highly sought-after. Dexrazoxane is hydrophilic and as a result has poor BBB penetration (36). However, there is a vast (and very desirable) amount of research into assisting larger drug molecules to cross the BBB. This research includes the co-administration of a bradykinin agonist which increases the permeability of the BBB allowing the drug of interest to pass into the brain compartment (37). An increasingly popular area of research, nanotechnology, may also allow passage of drugs across the BBB and in addition specific brain tumour targeting (38).

Our results in both cell types demonstrate coincubation with CP94 produces the greatest amount of PpIX fluorescence in the order MAL>ALA>HAL. Markedly, U-87 MG cells produced much greater levels of PpIX fluorescence than the A431 cells with all three prodrugs. Cell types show variability in their PpIX accumulation probably due to differences in their ferrochelatase activity which varies between cell types (6, 39). Ferrochelatase converts PpIX to heme by inserting a Fe^{2+} into the protoporphyrin ring. Thus, although not investigated here, if U-87 MG cells have a lower activity of the ferrochelatase enzyme than A431 cells and a higher metabolic rate, this could explain why over the same incubation period U-87 MG cells produce greater levels of PpIX fluorescence.

The objective of this study was to compare the effects of two iron chelating agents in combination with the porphyrin precursors ALA/MAL/HAL. For both cell types coincubation with CP94 produced a greater enhancement of PpIX accumulation than coincubation with dexrazoxane although this difference was most marked in the dermatological cells employed. The greatest amount of PpIX fluorescence was observed in the order MAL>ALA>HAL and the

same amount of PpIX fluorescence normally produced during 6 hour incubation with each prodrug alone was produced in shorter incubation times, when coincubated with CP94, achieved in the order HAL<ALA<MAL. In conclusion, although the enhancement of PpIX accumulation for different cell types may require different PpIX precursors or iron chelator combinations, this study has demonstrated that for ALA/MAL/HAL-induced PpIX production, enhancement can be successfully achieved with iron chelation and provides further evidence for the combined clinical investigation of this method of PDT/FGR enhancement.

REFERENCES

1. Pass, H.I. (1993) Photodynamic therapy in oncology: mechanisms and clinical use. *J Natl Cancer Inst*, **85**, 443-56.
2. Liu, H.F., S.Z. Xu, and C.R. Zhang (2004) Influence of CaNa2 EDTA on topical 5-aminolaevulinic acid photodynamic therapy. *Chin Med J (Engl)*, **117**, 922-6.
3. Szeimies, R.M., P. Calzavara-Pinton, S. Karrer, B. Ortel, and M. Landthaler (1996) Topical photodynamic therapy in dermatology. *J Photochem Photobiol B*, **36**, 213-9.
4. Pye, A., Y. Dogra, J. Tyrrell, P. Winyard, and A. Curnow, Redox Signaling and Regulation in Biology and Medicine, in Photodynamic Therapy with Aminolevulinic Acid and Iron Chelators: A Clinical Example of Redox Signaling, C. Jacob and P. Winyard, Editors. 2009, WILEY-VCH. p. 351-372.
5. Dailey, H.A. and A. Smith (1984) Differential interaction of porphyrins used in photoradiation therapy with ferrochelatase. *Biochem J*, **223**, 441-5.

6. el-Sharabasy, M.M., A.M. el-Waseef, M.M. Hafez, and S.A. Salim (1992) Porphyrin metabolism in some malignant diseases. *Br J Cancer*, **65**, 409-12.

7. Gibson, S.L., D.J. Cupriks, J.J. Havens, M.L. Nguyen, and R. Hilf (1998) A regulatory role for porphobilinogen deaminase (PBGD) in delta-aminolaevulinic acid (delta-ALA)-induced photosensitization? *Br J Cancer*, **77**, 235-42.

8. Kennedy, J.C., R.H. Pottier, and D.C. Pross (1990) Photodynamic therapy with endogenous protoporphyrin : IX: Basic principles and present clinical experience. *Journal of Photochemistry and Photobiology B: Biology*, **6**, 143-148.

9. Rhodes, L.E., M. de Rie, Y. Enstrom, R. Groves, T. Morken, V. Goulden, G.A. Wong, J.J. Grob, S. Varma, and P. Wolf (2004) Photodynamic therapy using topical methyl aminolevulinate vs surgery for nodular basal cell carcinoma: results of a multicenter randomized prospective trial. *Arch Dermatol*, **140**, 17-23.

10. Curnow, A. and A. Pye (2007) Biochemical manipulation via iron chelation to enhance porphyrin production from porphyrin precursors. *J Environ Pathol Toxicol Oncol*, **26**, 89-103.

11. Muller, P.J. and B.C. Wilson (2006) Photodynamic therapy of brain tumors--a work in progress. *Lasers Surg Med*, **38**, 384-9.

12. Frieboes, H.B., J.S. Lowengrub, S. Wise, X. Zheng, P. Macklin, E.L. Bearer, and V. Cristini (2007) Computer simulation of glioma growth and morphology. *NeuroImage*, **37**, 59-70.

13. Madsen, S.J., C.H. Sun, B.J. Tromberg, V.P. Wallace, and H. Hirschberg (2000) Photodynamic therapy of human glioma spheroids using 5-aminolevulinic acid. *Photochem Photobiol*, **72**, 128-34.

14. Stummer, W., S. Stocker, A. Novotny, A. Heimann, O. Sauer, O. Kempski, N. Plesnila, J. Wietzorrek, and H.J. Reulen (1998) In vitro and in vivo porphyrin accumulation by C6 glioma cells after exposure to 5-aminolevulinic acid. *J Photochem Photobiol B*, **45**, 160-9.

15. von Beckerath, M., P. Juzenas, L.W. Ma, V. Iani, L. Lofgren, and J. Moan (2001) The influence of UV exposure on 5-aminolevulinic acid-induced protoporphyrin IX production in skin. *Photochem Photobiol*, **74**, 825-8.

16. Kaneko, S. (2008) Recent advances in PDD and PDT for malignant brain tumours. *The Review of Laser Engineering*, 1351-1354.

17. Stummer, W., S. Stocker, S. Wagner, H. Stepp, C. Fritsch, C. Goetz, A.E. Goetz, R. Kiefmann, and H.J. Reulen (1998) Intraoperative detection of malignant gliomas by 5-aminolevulinic acid-induced porphyrin fluorescence. *Neurosurgery*, **42**, 518-25; discussion 525-6.

18. Chang, S.C., A.J. MacRobert, J.B. Porter, and S.G. Bown (1997) The efficacy of an iron chelator (CP94) in increasing cellular protoporphyrin IX following intravesical 5-aminolaevulinic acid administration: an in vivo study. *J Photochem Photobiol B*, **38**, 114-22.

19. Pye, A. and A. Curnow (2007) Direct comparison of delta-aminolevulinic acid and methyl-aminolevulinate-derived protoporphyrin IX accumulations potentiated by desferrioxamine or the novel hydroxypyridinone iron chelator CP94 in cultured human cells. *Photochem Photobiol*, **83**, 766-73.

20. Hanania, J. and Z. Malik (1992) The effect of EDTA and serum on endogenous porphyrin accumulation and photodynamic sensitization of human K562 leukemic cells. *Cancer Lett*, **65**, 127-31.

21. Sandeman, D.R., R. Bradford, P. Buxton, S.G. Bown, and D.G. Thomas (1987) Selective necrosis of malignant gliomas in mice using photodynamic therapy. *Br J Cancer*, **55**, 647-9.

22. Junjing, Z., Z. Yan, and Z. Baolu (2010) Scavenging effects of dexrazoxane on free radicals. *J Clin Biochem Nutr*, **47**, 238-45.

23. Buss, J.L. and B.B. Hasinoff (1995) Ferrous ion strongly promotes the ring opening of the hydrolysis intermediates of the antioxidant cardioprotective agent dexrazoxane (ICRF-187). *Arch Biochem Biophys*, **317**, 121-7.

24. Blake, E. and A. Curnow (2010) The Hydroxypyridinone Iron Chelator CP94 Can Enhance PpIX-induced PDT of Cultured Human Glioma Cells. *Photochem Photobiol*, **86**, 1154-60.

25. Curnow, A., B.W. McIlroy, M.J. Postle-Hacon, J.B. Porter, A.J. MacRobert, and S.G. Bown (1998) Enhancement of 5-aminolaevulinic acid-induced photodynamic therapy in normal rat colon using hydroxypyridinone iron-chelating agents. *Br J Cancer*, **78**, 1278-82.

26. Campbell, S.M., C.A. Morton, R. Alyahya, S. Horton, A. Pye, and A. Curnow (2008) Clinical investigation of the novel iron-chelating agent, CP94, to enhance topical photodynamic therapy of nodular basal cell carcinoma. *Br J Dermatol*, **159**, 387-93.

27. Peng, Q., A.M. Soler, T. Warloe, J.M. Nesland, and K.E. Giercksky (2001) Selective distribution of porphyrins in skin thick basal cell carcinoma after topical application of methyl 5-aminolevulinate. *J Photochem Photobiol B*, **62**, 140-5.

28. Dawson, K.M. (1975) Studies on the stability and cellular distribution of dioxopiperazines in cultured BHK-21S cells. *Biochem Pharmacol*, **24**, 2249-53.

29. Hasinoff, B.B. (1990) The hydrolysis activation of the doxorubicin cardioprotective agent ICRF-187 [+)-1,2-bis(3,5-dioxopiperazinyl-1-yl)propane). *Drug Metab Dispos*, **18**, 344-9.

30. Hasinoff, B.B. (1994) Pharmacodynamics of the hydrolysis-activation of the cardioprotective agent (+)-1,2-bis(3,5-dioxopiperazinyl-1-yl)propane. *J Pharm Sci*, **83**, 64-7.

31. Hasinoff, B.B., F.X. Reinders, and V. Clark (1991) The enzymatic hydrolysis-activation of the adriamycin cardioprotective agent (+)-1,2-bis(3,5-dioxopiperazinyl-1-yl)propane. *Drug Metab Dispos*, **19**, 74-80.

32. Hasinoff, B.B. (1993) Enzymatic ring-opening reactions of the chiral cardioprotective agent (+) (S)-ICRF-187 and its (-) (R)-enantiomer ICRF-186 by dihydropyrimidine amidohydrolase. *Drug Metab Dispos*, **21**, 883-8.

33. Hasinoff, B.B. (1990) The iron(III) and copper(II) complexes of adriamycin promote the hydrolysis of the cardioprotective agent ICRF-187 ((+)-1,2-bis(3,5-dioxopiperazinyl-1-yl)propane). *Agents Actions*, **29**, 374-81.

34. Valdes, P.A., K. Samkoe, J.A. O'Hara, D.W. Roberts, K.D. Paulsen, and B.W. Pogue Deferoxamine iron chelation increases delta-aminolevulinic acid induced protoporphyrin IX in xenograft glioma model. *Photochem Photobiol*, **86**, 471-5.

35. Fredenburg, A. M., R. K. Sethi, D. D. Allen and R. A. Yokel (1996) The pharmacokinetics and blood-brain barrier permeation of the chelators 1,2 dimethly-, 1,2 diethyl-, and 1-[ethan-1'ol]-2-methyl-3-hydroxypyridin-4-one in the rat. *Toxicology,* **108,** 191-9.

36. Hofland, K. F., A. V. Thougaard, M. Dejligbjerg, L. H. Jensen, P. E. G. Kristjansen, P. Rengtved, M. Sehested and P. B. Jensen (2005) Combining etoposide and dexrazoxane synergizes with radiotherapy and improves survival in mice with central nervous system tumors. *Clin Cancer Res*, **11**, 6722-29.

37. Inamura, T. and K. L. Black (1994) Bradykinin selectively opens blood-brain barrier in tumors. *J Cerebral Blood Flow Metabolism*, **14**, 862-70.

38. Brigger, I., J. Morizet, G. Aubert, H. Chacun, M-J. Terrier-Lacombe, P. Couvreur and G. Vassal (2002) Poly(ethylene glycol)-coated hexadecylcyanoacrylate nanospheres display a combined effect for brain tumour targeting. *JPET*, **303**, 928-36

39. Bartosova, J. and Z. Hrkal (2000) Accumulation of protoporphyrin-IX (PpIX) in leukemic cell lines following induction by 5-aminolevulinic acid (ALA). *Comp Biochem Physiol C Toxicol Pharmacol*, **126**, 245-52.

FIGURE CAPTIONS

Figure 1: Dark toxicity of the test compounds, CP94 (150 µM) and dexrazoxane (50 & 150 µM), incubated with A431 and U-87 MG cells alone. Cell viability is presented as a percentage

of the blank control cells incubated with modified EMEM alone. Bars indicate the mean of 3 wells with 1 standard deviation.

Figure 2: PpIX fluorescence in A431 cells incubated with (a) 250 µM ALA, (b) 1000 µM MAL, (c) 10 µM HAL alone or in combination with CP94 (150 µM) or dexrazoxane (50 & 150 µM), as a function of time. A statistical significant difference in PpIX fluorescence from the prodrug only incubated control cells is indicated by * ($p<0.05$). A statistically significant difference between cells incubated with CP94 and 50 µM dexrazoxane is indicated by + ($p<0.05$) and a statistically significant difference between cells incubated with CP94 and 150 µM dexrazoxane is indicated by Δ ($p<0.05$). Times for chelator incubated cells to achieve comparable levels of fluorescence to the ALA/MAL/HAL alone treated cells at 6 hr, indicated by the hashed lines on panels (a) – (c), are presented in (d).

Figure 3: PpIX fluorescence in U-87 MG cells incubated (a) 250 µM ALA, (b) 1000 µM MAL, (c) 10 µM HAL alone or in combination with CP94 (150 µM) or dexrazoxane (50 & 150 µM), as a function of time. A statistical significant difference in PpIX fluorescence from the prodrug only incubated control cells is indicated by * ($p<0.05$). A statistically significant difference between cells incubated with CP94 and 50 µM dexrazoxane is indicated by + ($p<0.05$) and a statistically significant difference between cells incubated with CP94 and 150 µM dexrazoxane is indicated by Δ ($p<0.05$). Times for chelator incubated cells to achieve comparable levels of fluorescence to the ALA/MAL/HAL alone treated cells at 6 hr, indicated by the hashed lines on panels (a) – (c), are presented in (d).

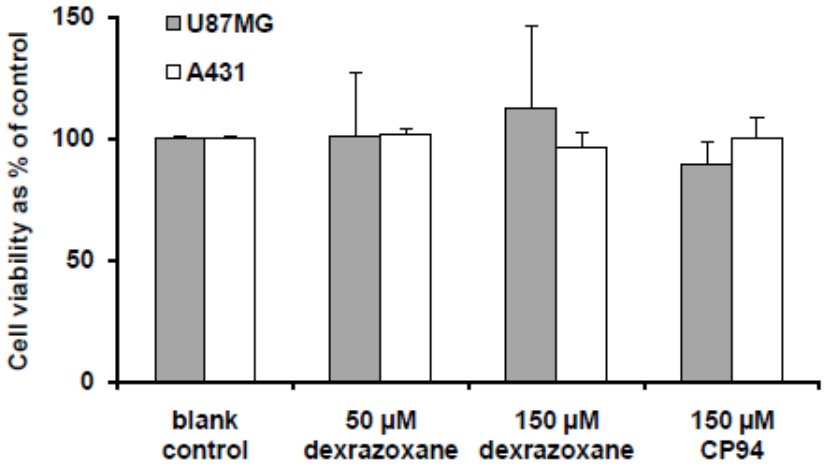
150
100
50
0
Cell viability as % of control
U87MG
A431
blank control
50 µM dexrazoxane
150 µM dexrazoxane
150 µM CP94

Figure 1.

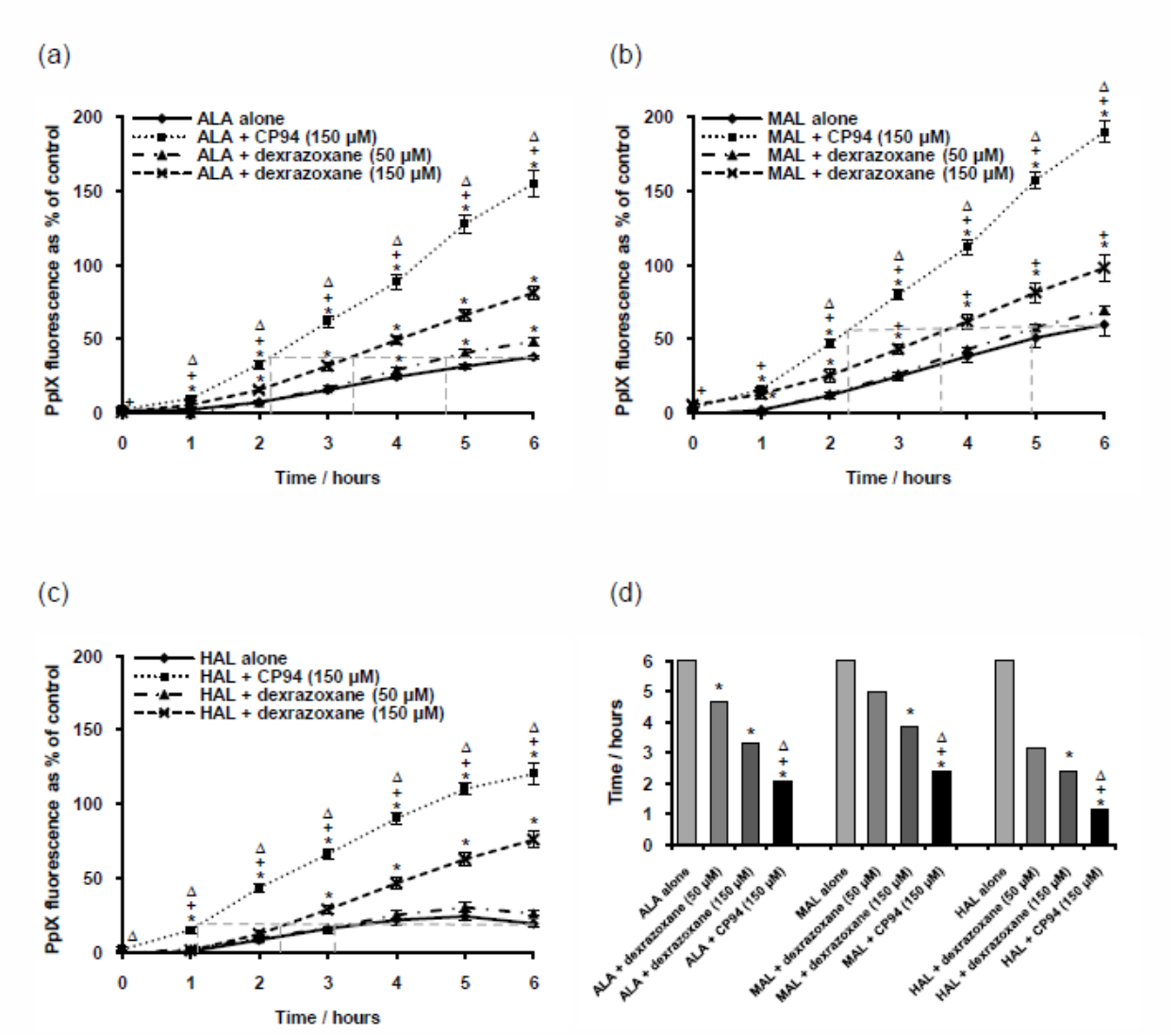
(a)
ALA alone
ALA + CP94 (150 µM)
ALA + dexrazoxane (50 µM)
ALA + dexrazoxane (150 µM)
PpIX fluorescence as % of control
Time / hours
(b)
MAL alone
MAL + CP94 (150 µM)
MAL + dexrazoxane (50 µM)
MAL + dexrazoxane (150 µM)
PpIX fluorescence as % of control
Time / hours
(c)
HAL alone
HAL + CP94 (150 µM)
HAL + dexrazoxane (50 µM)
HAL + dexrazoxane (150 µM)
PpIX fluorescence as % of control
Time / hours
(d)
Time / hours
ALA alone
ALA + dexrazoxane (50 µM)
ALA + dexrazoxane (150 µM)
ALA + CP94 (150 µM)
MAL alone
MAL + dexrazoxane (50 µM)
MAL + dexrazoxane (150 µM)
MAL + CP94 (150 µM)
HAL alone
HAL + dexrazoxane (50 µM)
HAL + dexrazoxane (150 µM)
HAL + CP94 (150 µM)

Figure 2.

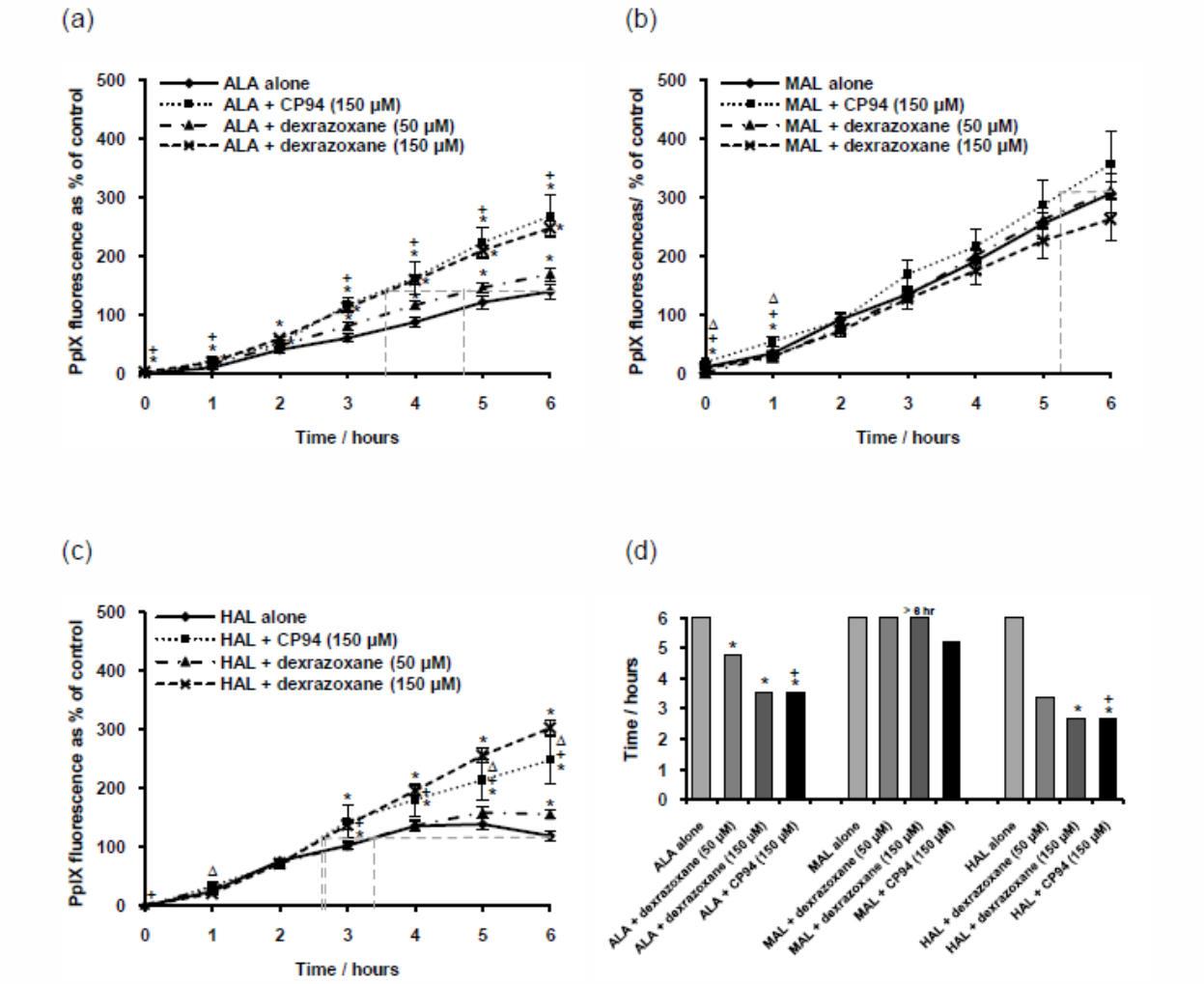
(a)
ALA alone
ALA + CP94 (150 µM)
ALA + dexrazoxane (50 µM)
ALA + dexrazoxane (150 µM)
PpIX fluorescence as % of control
Time / hours
(b)
MAL alone
MAL + CP94 (150 µM)
MAL + dexrazoxane (50 µM)
MAL + dexrazoxane (150 µM)
PpIX fluorescenceas/ % of control
Time / hours
(c)
HAL alone
HAL + CP94 (150 µM)
HAL + dexrazoxane (50 µM)
HAL + dexrazoxane (150 µM)
PpIX fluorescence as % of control
Time / hours
(d)
Time / hours
> 8 hr
ALA alone
ALA + dexrazoxane (50 µM)
ALA + dexrazoxane (150 µM)
ALA + CP94 (150 µM)
MAL alone
MAL + dexrazoxane (50 µM)
MAL + dexrazoxane (150 µM)
MAL + CP94 (150 µM)
HAL alone
HAL + dexrazoxane (50 µM)
HAL + dexrazoxane (150 µM)
HAL + CP94 (150 µM)

Figure 3.